Research Article | Vol. 28, No. 18 / 31 August 2020 / Optics Express 26067
Optics EXPRESS

# High resolution temperature sensor based on frequency beating between twin DFB fiber lasers

LAURENT DUSABLON,[1,*] VINCENT FORTIN,[1] TOMMY BOILARD,[1] MARTIN BERNIER,[1] PIERRE GALARNEAU,[2] FRANÇOIS BABIN,[2] AND RÉAL VALLÉE[1]

[1]Centre d'Optique, Photonique et Laser (COPL), Université Laval, Québec, G1 V 0A6, Canada
[2]INO, 2740 Einstein Street, Québec, G1P 4S4, Canada
[*]laurent.dusablon.1@ulaval.ca

**Abstract:** We present a high resolution temperature sensor using the beat frequency between the longitudinal modes of twin single-mode distributed feedback fiber lasers. The lasers are made by femtosecond inscription of π-shifted fiber Bragg gratings in a thulium-doped fiber. Combining the light from two single frequency fiber lasers on a photodetector produces a rf beat frequency signal which is dependent on temperature. Experimental results show a sensitivity of 1900 MHz/°C, leading to a precision of 0.0007 °C.



## 1. Introduction

Optical fiber sensors represent an active research area due to their superior properties and because of their very versatile sensing schemes. Optical fibers allow for robust, precise and distributed sensing over long distances, free of electromagnetic interference. Using different fiber structures and architectures such as fiber Bragg gratings (FBGs), Photonic Crystal Fibers (PCF), Fabry-Pérot interferometers, Mach-Zenhder interferometers and ring cavities allows for various parameters to be detected, such as temperature, strain, refractive index and vibrations. [1–6]. When very high resolution is required, interferometric sensors are generally preferred. For instance, strain measurements down to 270 pε [7] and temperature measurement down to $6 \times 10^{-4}$ °C [8] can be obtained.

When two slightly different optical frequencies mix on a standard photodetector, their difference gives rise to a detectable radio-frequency (rf) beat frequency. This signal can be used to probe physical or chemical properties. Kim et al. proposed this method in 1993, using the different polarization modes of a fiber laser [9]. Since the detection is in the rf domain, there is no need for a costly or bulky Optical Spectrum Analyzer (OSA). Beat frequency measurements can be done with passive components, like FBGs, but is often improved by using in situ lasing sources made of doped fibers (an approach known as active sensing). Active sensing benefits from a high signal to noise ratio, locally generated optical signals and narrow linewidths. Several designs have been investigated using frequency beating between the modes of a single laser [2,10]. Different physical properties that affect a fiber laser such as temperature or strain can be discriminated and measured by using the different sensitivity of polarization modes and longitudinal modes through rf beat measurements or through measurement of absolute optical frequency (wavelength) [11–13]. Using the rf beat frequencies generated by a fiber laser as a sensing signal is thus a very powerful approach which can be used for detection of temperature, lateral force, hydrostatic pressure, strain, ultrasound, bending, displacement, acceleration or current [14].

Alternatively, using two lasers, it is possible to look at the variation in the frequency value of a single longitudinal mode instead of the variation of the difference between two successive modes from the same source, potentially greatly enhancing the sensitivity. Single-frequency fiber lasers (SFFL) are well suited for this because they have very narrow linewidths and are immune to

#395949 https://doi.org/10.1364/OE.395949
Journal © 2020 Received 1 May 2020; revised 30 Jul 2020; accepted 6 Aug 2020; published 20 Aug 2020

Optics EXPRESS

mode-hopping [15]. One laser acts as a reference, while the second laser acts as the actual sensor [7]. This detection scheme was proposed in 2012 with a ring SFFL and a tunable reference laser for temperature measurements [15]. A version of this scheme was recently produced by Duan et al. who reported a sensitivity of 1832 MHz/°C with a temperature resolution of 0.005 °C [16].

In this paper, a temperature sensor using the beat frequency variation between two twin single longitudinal mode Distributed Feedback (DFB) lasers (made using the same parameters) is proposed. The lasers are made of 1.4 cm long π-shifted FBGs inscribed in a thulium doped fiber, making this the first heterodyne sensor using thulium. Thulium fibers are interesting both for their ability to obtain higher wavelength and for their increased thermal coefficient due to the inclusions of $Al_2O_3$. [17] The beat frequency is obtained by combining the laser outputs through a 50/50 coupler. This highly sensitive sensor uses locally generated signals for heterodyne detection in the rf spectral domain. The DFBs are easy to produce and to use, making this a very simple, all-fiber, low cost sensor with great potential for a multitude of uses, such as differential temperature measurements and temperature insensitive strain or curvature measurements. The sensor achieves a sensitivity of 1900 MHz/°C and precision of $7 \times 10^{-4}$°C, which is amongst the best heterodyne sensing schemes reported to date.

## 2. Detection setup

The π-shifted FBG inscribed in the gain fiber essentially acts like two concatenated FBGs, thus forming a Fabry-Pérot cavity [18]. In such cavity, the frequencies of longitudinal modes are determined by $\upsilon = \frac{qc}{2nL}$, where c is the speed of light, L the length, n the refractive index of the cavity and q is the mode number. As can be seen, a change in n or L yields a proportional change δν in frequency. However, a small change in the nominal frequency ν is hard to detect with an OSA, as δν is usually a very small fraction of ν.

When two lasers with carrier frequencies $\nu_1$ and $\nu_2$ are combined, the detected beat frequency is $\nu_1$-$\nu_2$. If $\nu_1$ changes by a value δν, whereas $\nu_2$ is kept constant, the beat frequency also changes by the same amount δν. However, since the change is detected using the beat frequency, it represents a larger relative change in the rf domain than in the optical domain, i.e. $\delta\nu/(\nu_1-\nu_2) >> \delta\nu/\nu$. Typically, one is comparing a change of 100 MHz over 1 GHz instead of over 100 THz.

The experimental setup is illustrated in Fig. 1. Two twin thulium doped DFB lasers are in-band pumped by a fiber laser at 1580 nm.

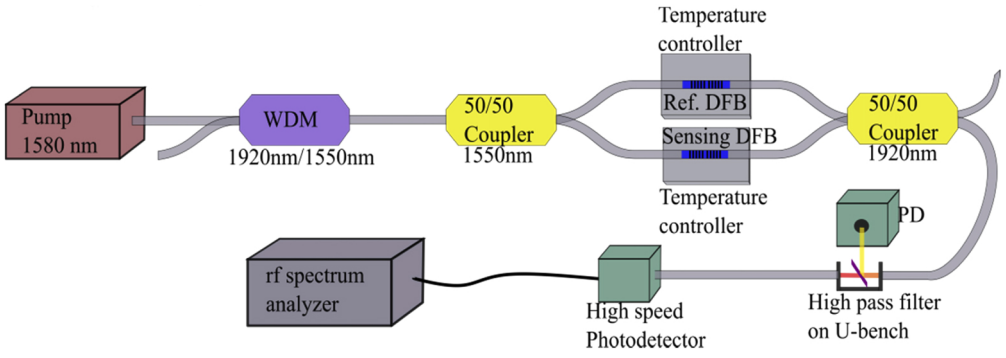


**Fig. 1.** Experimental setup of the sensor.

The pump laser is a 450 mW in-house made erbium-doped 1580 nm fiber laser [19]. The pump light is launched into the 1920/1550 nm division wavelength multiplexer (WDM). The WDM is introduced to act as a rejection filter for the DFB laser light that is emitted in the backwards direction, therefore preventing the destabilization of the pump and allowing the monitoring of

Optics EXPRESS

the DFB lasers. The pump light is then split with a 50/50 coupler at 1550 nm so that the DFB lasers equally share the pump power. The DFB lasers, which are further described below, are each placed on independent temperature controlled metal blocks, which allow precise control of their temperature. A second metal block is placed on top of the fiber sensors. Thermal paste is added in between the blocks for good thermal contact. This setup somewhat isolates the sensors from environmental fluctuations. The output from the DFB lasers are then combined via a 50/50 coupler operating at 1920 nm, allowing them to overlap in the core of the fiber. The residual pump is then removed by a long pass filter mounted on a U-bench. The resulting signal is finally sent directly onto a fast photodetector (12.5 GHz ET-5000F from EOTech) connected to a rf spectrum analyzer, (either 10 GHz Infiniium oscilloscope from Agilent or 3 GHz Gen3 EON Express analyzer from GaGe).

## 3. DFB lasers

The DFB fiber lasers provide both the sensing and the reference signals. Using an 800 nm femtosecond laser and the scanning phase mask technique [20], 1.4 cm π-shifted FBGs were inscribed in 2.5 cm of thulium doped fiber. The gratings were engineered so that their spectral widths are significantly smaller than the distance between two consecutive longitudinal modes, leading to single frequency lasing. The active fiber (CorActive, DCF-TM-9/128P-13) is heavily doped with thulium, allowing for high absorption in a short length (143 dB/m core pump absorption at 1580 nm, 56% over the cavity length). This fiber can also be spliced to a SMF-28 fiber with minimal mode-matching losses. During the experiment, the DFBs are core-pumped by the same 1580 nm fiber laser. Each DFB is pumped with 225 mW at 1580 nm and emits approximately 1 mW at both ends. The laser threshold is at 30 mW of pump power.

Each DFB's spectrum was measured with an OSA and a Fabry-Pérot interferometer. As can be seen in Fig. 2(a), both DFBs are spectrally very close to each other, emitting near 1922.3 nm. However, the OSA's resolution (0.08 nm) is not sufficient to ascertain single longitudinal mode emission. The DFB's spectra were then analyzed using a scanning Fabry-Pérot interferometer (Thorlabs SA210-18C).

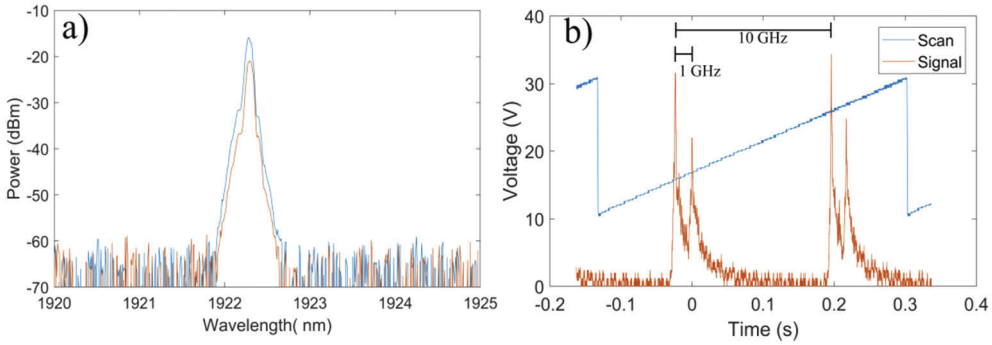


**Fig. 2.** a) Optical emission spectrum of both DFBs b) Scanning Fabry-Pérot interferometer trace

As can be seen in Fig. 2(b), there are two modes separated by 1 GHz, corresponding to the two polarization modes for each DFB. In fact, since our fibers are not polarization maintaining, the DFB emits light in two polarization modes. The beat frequency from these modes can be measured with the photodetector and the rf spectrum analyzer and vary depending on the DFB. These beat frequencies were simply discarded here at the signal processing step. Since no other mode was detected with the scanning Fabry-Pérot interferometer, it is assumed that the lasers are emitting in a single longitudinal mode. Using the temperature controller to change

Optics EXPRESS

the temperature, one DFB's optical frequency was scanned across the other laser's frequency. No other beat frequencies were seen except those expected from two DFB lasers with only one longitudinal mode and two polarization modes each.

Figure 3 shows the beat signal between the two polarization modes of a single DFB laser. The linewidth is 11.4 kHz at -10 dB. Assuming a Lorentzian lineshape, full width at half maximum (FWHM) is 3.8 kHz. It is assumed that both modes have similar linewidths. Since the modes shift slightly during data acquisition (1.33 ms at $3 \times 10^9$ samples/s with a Gen3 EON express analyzer from GaGe), the value 3.8 kHz actually represents an upper bound for the mode linewidth.

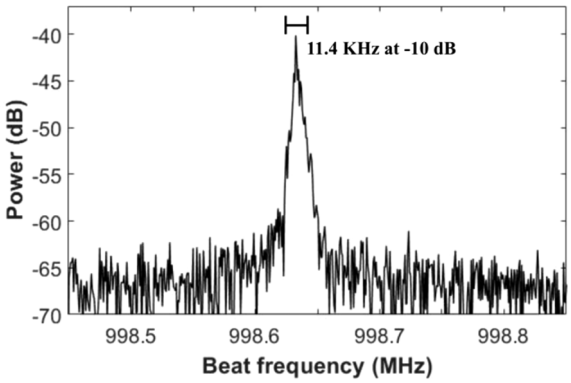


**Fig. 3.** Linewidth of polarization beat frequency of a single laser

## 4. Results and analysis

The DFB lasers are mounted on temperature controlled blocks. The fiber is sandwiched between a metallic groove and a metallic cover, and is surrounded by thermal paste to ensure good thermal contact between the fiber and its surrounding. The metallic block with a groove is on top of a thermo-electric cooler (TEC), and the temperature is measured with a thermistor. The temperature is regulated by a temperature controller (Wavelength Electronics MPT-5000). This yields a high temperature stability over time and also allowed control over the temperature of the fiber sensor. The temperature of the block over which one DFB laser is mounted was gradually increased from 15 °C to 20 °C, leaving the temperature controller enough time to stabilize the temperature between each measurement. The other DFB laser was kept at constant temperature using another temperature controller (ILX lightwave LDT-5940C). No stress was applied to the fibers.

The signal is analyzed using an rf analyzer. The Fourier transform is processed to get rid of sampling artifacts and the beat modes can be easily measured as the temperature changes. In Fig. 4(a) a typical experimental rf spectrum analyzed at 3 GS/s is presented. In Fig. 4(b), a schematic is shown where red peaks represent the polarization modes of the sensing laser, which move as temperature is increased during the experiment, and blue peaks represent the polarization modes of the reference laser, which remain stable. The first peak on Fig. 4(a) (546 MHz) is the beat frequency between the two laser's longitudinal modes, identified by $\boldsymbol{\omega_1}$ in the Fig. 4(b). The second peak (1010 MHz) is the beat mode between one laser's polarization modes, identified by $\mathbf{P_1}$. The third peak (1444 MHz) corresponds to the beating between one laser's main longitudinal mode and the other laser's polarization mode at 1556 MHz, folded over the Nyquist frequency, identified by $\boldsymbol{\omega_2}$. Not appearing in Fig. 4(a) are the second laser's polarization mode beating ($\mathbf{P_2}$) and the other beating between the polarization modes of the lasers ($\boldsymbol{\omega_3}$ and $\boldsymbol{\omega_4}$). Their

Optics EXPRESS

frequencies are significantly higher than the sampling frequency. $\mathbf{P_1}$ and $\mathbf{P_2}$ are beating between polarization modes and as such do not vary as temperature is increased.

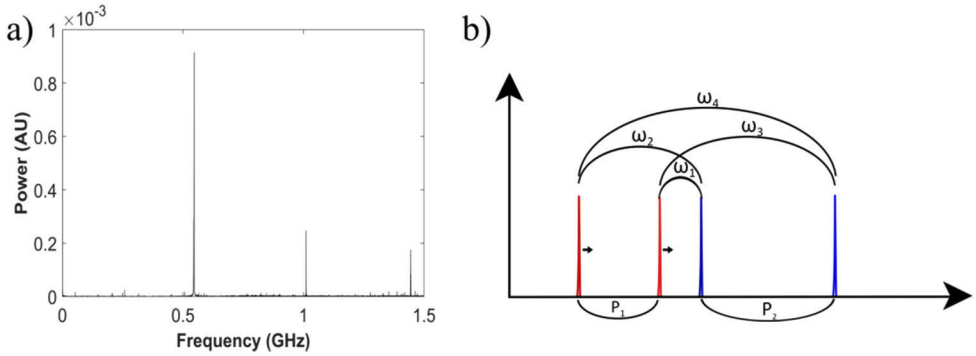


**Fig. 4.** a) Example of a beat frequency spectrum for an acquisition of 13 µs at 3 GS/s b) Schematic of the laser modes of the reference and sensing DFBs. Red peaks represent the polarization modes of the sensing laser and blue peaks the polarization modes of the reference laser.

Beat frequency $\boldsymbol{\omega_1}$ was tracked by an rf analyzer at 20 GS/s as the temperature of the sensing DFB was changed whereas the reference DFB laser was stabilized at 18 °C.

As can be seen in Fig. 5, a linear relation between the temperature and the beat frequency is observed. The temperature was scanned from 14.97 °C to 20.11 °C, corresponding to a beat frequency shift from -5796 MHz to 4178 MHz. Positive/negative values are used to signify the wavelength of the sensing laser was either lower or higher than that of the reference laser. A linear fit on the data yields a slope of 1900 MHz/°C with a root mean square (RMS) deviation of 150 MHz. This also corresponds to a slope of 23.4 pm/°C at 1922 nm. This slope was confirmed over a broader temperature range (from 15 to 35 °C) using an optical spectrum analyzer (Yokogawa AQ6376), where the slope $\Delta\lambda/\Delta T$ is 26.6 pm/°C over 25°C (cf. Figure 6). The temperature dynamical range is determined by the photodetector's bandwidth. With the fast photodetector from EOTech that was used, the temperature dynamical range is 13 °C or ± 6.5 °C around the temperature set by the reference DFB.

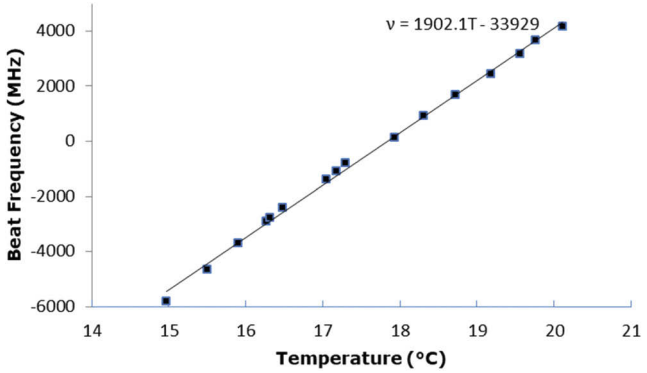


**Fig. 5.** Beat frequency as a function of temperature for one DFB laser acting as a sensor

Assuming the previously derived linewidth of 3.8 kHz as our resolution limit, the corresponding temperature resolution would be $2 \times 10^{-6}$ °C. However, the precision of the sensor is ultimately limited not by the instantaneous linewidth of the individual DFBs but rather by their long-term

Optics EXPRESS

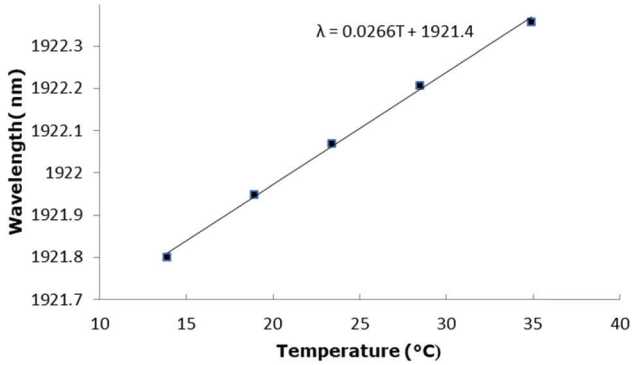


**Fig. 6.** Wavelength shift measured with an optical spectrum analyzer

relative frequency drift. Figure 7 shows the beat frequency linewidth for a typical measurement and illustrates the noise for a single measurement acquired over 133 µs. A -10 dB linewidth of 300 KHz is obtained, which is significantly larger than the 11.4kHz linewidth previously obtained with two polarisation modes from the same DFB (cf. Figure 3).

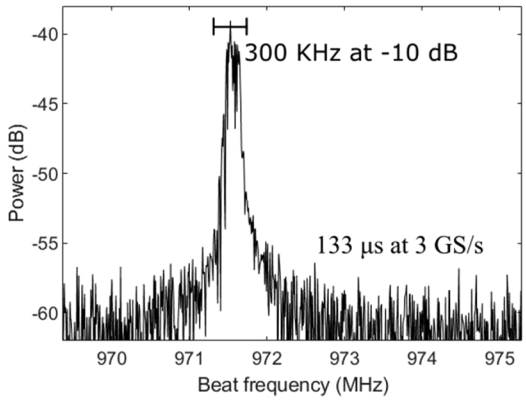


**Fig. 7.** Beat frequency linewidth for a single measurement

We further investigated the stability of the beat signal over a longer time interval. Accordingly, we noted a long-term frequency jitter of the beat frequency which is believed to be due to variations in external conditions, namely fluctuations of the pump power.

Beat frequency measurements were made every second by applying a Fast Fourier Transform (FFT) algorithm over time slots of 133 µs (at $3 \times 10^9$ samples/s), for a total of 60 entry points over a one minute duration (Fig. 8). In obtaining the preceding frequency jitter, the temperature of each DFB laser was kept constant and stabilized by each temperature controller. As can be seen in Fig. 8, the beat frequency value fluctuates with a peak to peak jitter of 6 MHz and a RMS value of 1.35 MHz, which is almost three orders of magnitude larger than the DFB linewidth. This RMS jitter actually limits the sensor precision to $7 \times 10^{-4}$ °C.

We also investigated the role of the temperature controllers in the overall sensor's performances. First, we note that the temperature controllers used are specified to have a stability of 0.003 °C and 0.002°C over an hour. Now, to estimate the actual impact of the temperature controller fluctuations, we placed both DFBs on the same temperature controller, in such a way that they would be very close to each other. Jitter was then analyzed in the same manner as before. The

Optics EXPRESS

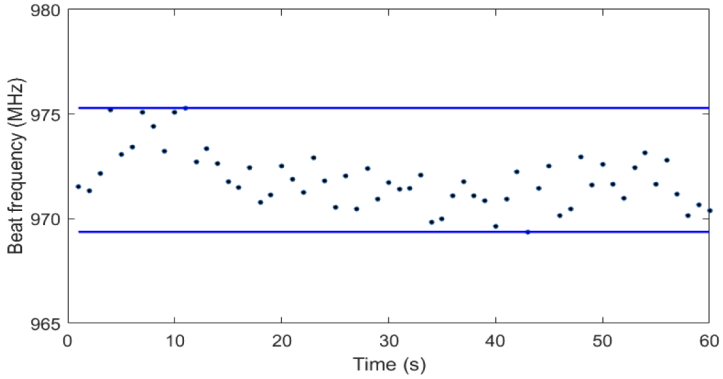


**Fig. 8.** Beat frequency jitter over a minute. Each point corresponds to a time acquisition of 133μs at 3 GS/s.

frequency jitter was then shown to improve by about 30%, which demonstrate that the TEC were indeed partly playing a role in limiting the precision of the sensor.

Sensitivity to pump power was also investigated. We measured that a change of 80 mW of total pump power led to a 113 MHz beat frequency shift. This results in a pump power sensitivity of 1.4 MHz/mW. Pump power fluctuations were investigated at the long pass filter at 10 samples/s and are given in Fig. 9. The RMS stability in this case is 0.3%, which represents a variation of 1.3 mW of total pump power. The beat frequency stability is therefore heavily influenced by pump power variations. It is thus concluded that improving pump stability would increase the precision of our sensing device.

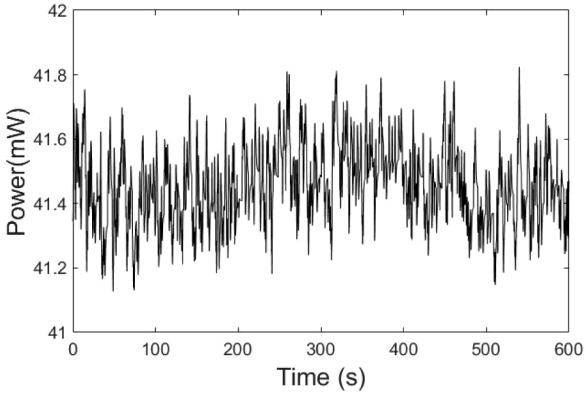


**Fig. 9.** Stability of pump power at the high-pass filter

Table 1 presents the sensitivity performance and the smallest discernible temperature change of different wavelength encoding temperature fiber sensors reported in the literature. As can be seen, some fiber sensing techniques are more sensitive than this paper's scheme. However, the corresponding setups usually involve complex components, a low signal to noise ratio or large linewidth, leading to poor resolution. With optical mode beating, the addition of a reference laser greatly enhances the sensitivity and resolution of measurements. The sensing scheme presented here has the greatest sensitivity of heterodyne beat schemes and has comparable performance with high resolution fiber temperature sensors. The DFB lasers used are easy to produce and simple to use. Precision being presently limited by the laser's optical frequency noise, it would

Optics EXPRESS

be possible to increase laser optical frequency stability by increasing pump stability, for example by an active feedback. Static strain, axial strain and bending measurement could also be made with slight alterations to the setup presented here. High resolution refractive index measurements and chemical detection could finally be performed based on this approach with an appropriate sensing scheme.

**Table 1. Performance comparison of wavelength encoding temperature sensors**

| Reference | Sensitivity | Smallest discernible ΔT | Sensing scheme |
|---|---|---|---|
| This paper | 23.4 pm/°C | $7\times10^{-4}$°C | Beating between twin single longitudinal mode DFB lasers |
| [16] | 14.74 pm/°C | 0.005°C | Beating between SFFL and reference laser |
| [15] | 10.4 pm/°C | 0.0023°C | Beating between SFFL and reference laser |
| [11] | 0.013 pm/°C | 0.04°C | Polarization beat frequency and absolute wavelength |
| [13] | 0.08 fm/°C | 1.0°C | Longitudinal mode beating of a single multimode laser |
| [12] | 0.011 pm/°C | 0.05°C | Polarization beat frequency and absolute wavelength |
| [21] | 20 pm/°C | 0.58°C | Miniaturized fiber taper reflective interferometer |
| [22] | 10.25 pm/°C | 0.001 °C | Slow-light fiber Bragg grating |
| [8] | 84.6 pm/°C | $6\times10^{-4}$ °C | Fabry-Pérot silicon pillar Tip |
| [23] | 9.74 pm/°C | $4.1\times10^{-4}$ °C | FBG and absolute frequency reference |
| [24] | 4.02 pm/°C | $1.1\times10^{-4}$°C | Efficient cavity length |

## 5. Conclusion

A high-resolution temperature sensor was presented. It uses twin DFB lasers and the measurements of the beat frequency between them. When the temperature was scanned from 15 to 20 °C, a sensitivity of 1900 MHz/°C was measured. In the current scheme, this represents a precision of $7\times10^{-4}$ °C, which could be further enhanced by increasing pump stability. The sensor allows locally generated laser signal to remotely measure temperature between two points or at a single point. The setup is versatile and with the proper detection system could be also used to get high resolution measurements of strain, bending, refractive index or analyte concentration.

## Funding

Natural Sciences and Engineering Research Council of Canada (CG112389, IRCPJ469414-13); Canada Foundation for Innovation (5180); Fonds de recherche du Québec – Nature et technologies (144616).

## Disclosures

The authors declare no conflict of interest.

## References

1. W. W. Morey, G. Meltz, and W. H. Glenn, "Fiber Optic Bragg Grating Sensors," Proc. SPIE **1169**, 98–107 (1989).
2. L. Gao, L. Chen, L. Huang, and X. Chen, "Multimode fiber laser for simultaneous measurement of strain and temperature based on beat frequency demodulation," Opt. Express **20**(20), 22517–22522 (2012).
3. D. N. Wang, H. Chen, and Y. Wang, "Selectively Infiltrated PCF for Directional Bend Sensing With Large Bending Range," IEEE Photonics Technol. Lett. **27**, 98 (2014).
4. X.-Y. Sun, D.-K. Chu, X.-R. Dong, H.-T. Chu-Zhou, Y.-W. Luo-Zhi Li, J.-Y. Hu, J.-A. Cong-Wang Zhou, and Duan, "Highly sensitive refractive index fiber inline Mach–Zehnder interferometer fabricated by femtosecond laser micromachining and chemical etching," Opt. Laser Technol. **77**, 11–15 (2016).
5. X. Wan and H. F. Taylor, "Intrinsic fiber Fabry–Perot temperature sensor with fiber Bragg grating mirrors," Opt. Lett. **27**(16), 1388–1390 (2002).

Optics EXPRESS


6. L. Gao, S. Liu, Z. Yin, L. Zhang, L. Chen, and X. Chen, "Fiber-Optic Vibration Sensor Based on Beat Frequency and Frequency-Modulation Demodulation Techniques," IEEE Photonics Technol. Lett. **23**(1), 18–20 (2011).
7. W. Huang, S. Feng, W. Zhang, and F. Li, "DFB fiber laser static strain sensor based on beat frequency interrogation with a reference fiber laser locked to a FBG resonator," Opt. Express **24**(11), 12321–12329 (2016).
8. G. Liu, M. Han, and W. Hou, "High-resolution and fast-response fiber-optic temperature sensor using silicon Fabry-Pérot cavity," Opt. Express **23**(6), 7237–7247 (2015).
9. H. Kim, S. Kim, H. Park, and B. Kim, "Polarimetric fiber laser sensors," Opt. Lett. **18**(4), 317–319 (1993).
10. G. Ball, G. Meltz, and W. Morey, "Polarimetric heterodyning Bragg-grating fiber-laser sensor," Opt. Lett. **18**(22), 1976–1978 (1993).
11. O. Hadeler, E. Rønnekleiv, M. Ibsen, and R. Laming, "Polarimetric distributed feedback fiber laser sensor for simultaneous strain and temperature measurements," Appl. Opt. **38**(10), 1953–1958 (1999).
12. L. Shao, X. Dong, A. P. Zhang, H. Tam, and S. He, "High-Resolution Strain and Temperature Sensor Based on Distributed Bragg Reflector Fiber Laser," IEEE Photonics Technol. Lett. **19**(20), 1598–1600 (2007).
13. Z. Yin, L. Gao, S. Liu, L. Zhang, F. Wu, L. Chen, and X. Chen, "Fiber Ring Laser Sensor for Temperature Measurement," J. Lightwave Technol. **28**, 3403–3408 (2010).
14. B. Guan, L. Jin, Y. Zhang, and H. Tam, "Polarimetric Heterodyning Fiber Grating Laser Sensors," J. Lightwave Technol. **30**(8), 1097–1112 (2012).
15. H. Ahmad, A. A. Latif, M. Z. Zulkifli, N. A. Awang, and S. W. Harun, "Temperature Sensing Using Frequency Beating Technique From Single-Longitudinal Mode Fiber Laser," IEEE Sens. J. **12**(7), 2496–2500 (2012).
16. L. Duan, H. Zhang, W. Shi, X. Yang, Y. Lu, and J. Yao, "High-Resolution Temperature Sensor Based on Single-Frequency Ring Fiber Laser via Optical Heterodyne Spectroscopy Technology," Sensors **18**(10), 3245 (2018).
17. M. Cavillon, P. D. Dragic, and J. Ballato, "Additivity of the coefficient of thermal expansion in silicate optical fibers," Opt. Lett. **42**(18), 3650–3653 (2017).
18. H. Kogelnik and C. V. Shank, "Coupled-wave theory of distributed feedback lasers," J. Appl. Phys. **43**(5), 2327–2335 (1972).
19. M. Lord, L. Talbot, O. Boily, T. Boilard, G. Gariépy, S. Grelet, P. Paradis, V. Boulanger, N. Grégoire, S. Morency, Y. Messaddeq, and M. Bernier, "Erbium-doped aluminophosphosilicate all-fiber laser operating at 1584 nm," Opt. Express **28**(3), 3378–3387 (2020).
20. J. Habel, T. Boilard, J.-S. Frenière, F. Trépanier, and M. Bernier, "Femtosecond FBG written through the coating for sensing applications," Sensors **17**(11), 2519 (2017).
21. J. Kou, J. Feng, L. Ye, F. Xu, and Y. Lu, "Miniaturized fiber taper reflective interferometer for high temperature measurement," Opt. Express **18**(13), 14245–14250 (2010).
22. A. Arora, M. Esmaeelpour, M. Bernier, and M. J. F. Digonnet, "High-resolution slow-light fiber Bragg grating temperature sensor with phase-sensitive detection," Opt. Lett. **43**(14), 3337–3340 (2018).
23. Q. W. Liu, J. G. Chen, X. Y. Fan, L. Ma, J. B. Du and Z, and Y. He, "Optical fiber temperature sensor with mK resolution and absolute frequency reference," Proc. SPIE **9655**, 965508 (2015).
24. W. Huang, W. Zhang, and F. Li, "Fiber Bragg grating resonator for ultrahigh-resolution temperature sensing based on efficient cavity length," in *26th International Conference on Optical Fiber Sensors, OSA Technical Digest* (Optical Society of America, 2018), paper TuE94.